Progress In Electromagnetics Research B, Vol. 90, 129–150, 2021

Electromagnetic Simulation for Estimation of Forest Vertical Structure Using PolSAR Data

Shimaa A. M. Soliman[1, *], Khalid F. A. Hussein[1], and Abd-El-Hadi A. Ammar[2]

Abstract—A novel method for the estimation of a forest vertical structure using Polarimetric Synthetic Aperture Radar (PolSAR) data only without the need to interferometry data is proposed in the present paper. Electromagnetic (EM) simulation is used to develop the proposed method, where the SAR pulse is simulated as a plane wave incident in the direction of the side looking angle of the SAR. For this purpose, the forest canopy layer is modeled as clouds of randomly oriented thin straight dipoles which are randomly distributed within an inclined prism volume, whereas the forest soil surface is modeled as a random rough surface. The proposed method aims to estimate the average height of the canopy layer above the soil surface, the canopy layer thickness, and the roughness of the forest ground surface. The proposed method is based on the Radar Vegetation Index (RVI) and the normalized Radar Cross Section (RCS) calculated from the PolSAR data and their relevance to the parameters of the forest vertical structure. Some examples are presented to demonstrate the capability of the proposed method using some PolSAR images obtained through EM simulation of the scattering from forest regions and by applying the theorem of SAR target composition with the Multiple Component Scattering Model (MCSM). The phase differences between the components of scattering obtained from the solution of the SAR target decomposition problem are used in the estimation process. The accuracy of the proposed method is assessed by calculating the percentage error of the estimated vertical structure and ground roughness for each resolution cell of the simulated forest region. It is shown that the percentage errors of the estimated parameters are very low, which reflects the accuracy and efficiency of the proposed method.

1. INTRODUCTION

Besides the economic and commercial importance of the forests that provide timber and wood, forest canopy layer has a great role in providing vital ecosystem services [1, 2]. Accordingly, the most common application in vegetation observation has become the estimation of the forest vertical structure with emphasis on accurate estimation of the canopy layer thickness.

In polarimetry, the radar measures, at the same time, S_{hh}, S_{vv}, S_{hv}, S_{vh} and their phase difference whereas in interferometry remote sensing, two radars observe the scene with a small shift in the look angle or the same radar at different dates from slightly shifted orbit. Polarimetric and interferometric synthetic aperture radar (PolInSAR) data inversion at L-band can be used to estimate forest heights [3–5]. Some recently published papers are concerned with developing methods based on PolInSAR data for the estimation of forest vertical structure. For example, the method described in [3] applies common techniques that use interferograms in multiple polarization channels to estimate vegetation height and underlying ground topography. The work of [4] is concerned with forest parameter retrieval from PolInSAR considering two-layer model of the forest structure. A model is designed

Received 8 November 2020, Accepted 5 January 2021, Scheduled 14 January 2021

* Corresponding author: Shimaa Ahmed Megahed Soliman (megahed.shaimaa@yahoo.com).

[1] Microwave Engineering Department, Electronics Research Institute (ERI), Cairo, Egypt. [2] Electronics and Electrical Communications Department, Faculty of Engineering, Al-Azhar University, Cairo, Egypt.

to combine a physical model-based polarimetric decomposition with the random-volume-over-ground (RVoG) PolInSAR parameter inversion approach. Also, PolInSAR techniques have been applied to retrieve the vegetation height based on the RVoG model [6, 7]. A method depending on the L-band PolInSAR data is presented in [2] to predict the canopy height and canopy cover through neuronal network learning. This method results in the estimated canopy height and canopy cover with normalized root-mean-squared errors of 13% and 15%, respectively [2].

It is known that the vegetation structure results in significant cross polarization of the backscattered field. The reasons for this are the random orientations of the tree branches and narrow long leaves existing in the vegetation regions and the multiple bounces of the incident microwave on the particles such as leaves and small branches which are randomly distributed within the vegetation structure. For a radar wavelength about 24 cm (L-band), the leaves and small branches of the trees do not contribute significantly to the backscattering. The branches whose length is in order of 20 cm or longer significantly contribute to the backscattering in the L-band. Due to their water content, such branches can be modeled as conductive thin straight dipoles. Most of the tree types usually have their branches pointing in random directions, so the canopy is modeled as randomly oriented straight thin dipoles with uniform random distribution in a cloud of a proper shape. The radar vegetation index (RVI) is a microwave metric of vegetation cover that is widely used to monitor vegetation growth and vegetation water content (VWC) [8–11].

The present paper is concerned with describing a new robust method to accurately estimate the forest vertical structure using the data available in the PolSAR images for the forested area under investigation. The proposed method makes use of the data collected by PolSAR (in one time) without the need of a shift in the look angle or shift in the measurement date. There is no need of interferometry in the proposed technique. This greatly simplifies the process of canopy layer thickness estimation. The proposed method is based on the RVI and normalized RCS which are calculated from the collected PolSAR data. In the analysis presented in this paper, it is shown that the RVI and normalized RCS are strongly dependent on the canopy layer thickness. The proposed method is based on some curves which are fitted to describe the dependence of these radar quantities on the canopy thickness and some other parameters such as the roughness degree of the ground surface beneath the trees.

Simulated coherent SAR data are commonly used for estimating the forest vertical structure [12–16]. To apply the method proposed in the present work, simulated SAR data sets are obtained for forest regions of a specific vertical structure that can be used for subsequent estimation process. This requires electromagnetic simulation of the SAR imaging operation where a plane wave is assumed to be incident on realistic geometric models for the forest canopy layer, the rough surface representing the soil surface beneath the trees, and the corners constituted by the vertical tree trunks and the horizontal ground. The theory of SAR target decomposition with the multiple component scattering model (MCSM) is then applied to get the backscattering from such a composite structure of the forest. Target decomposition with three-, four-, and five-component scattering models is described in [17–19], respectively. The three-component scattering model (volume scattering, single-bounce, and double-bounces) described in [17] is used in the present work for this purpose. The scattering coefficients representing the PolSAR data are, thus, obtained for the forest region. The proposed method is, then, applied to the simultaneous estimation of the canopy thickness, height, and ground roughness distribution over the forest region.

The accuracy of the proposed method is assessed by calculating the percentage errors of the estimated canopy thickness, height, and ground roughness for each cell of the simulated forest region. Some numerical examples are presented to demonstrate the capability of the proposed method to accurately estimate the forest vertical structure using PolSAR image obtained through EM simulation.

2. FOREST VERTICAL STRUCTURE

A forest is made up of several trees that belong to many species. A tree has a stem and a crown of branches that bear leaves, flowers, and fruits. The forest structure is commonly described in two directions:

- *Horizontal structure* is created by the placement of trees and how close their crowns are to each other. As shown in Figure 1, a collection of these crowns creates the canopy.

Figure 1. Layers of the common forest vertical structure.

- *Vertical structure* is formed because trees and shrubs in a forest have different heights as shown in Figure 1. So, two or more layers of tree crowns can be found in forests. These layers are called forest storeys or strata. The top-most stratum is made of the crowns of emergent trees; below them is the continuous canopy layer formed by the overlapped tree crowns. The tree strata below them are called the sub-canopy and understorey. Next, close to the ground could be shrubs, herbs, and grasses.

3. FREQUENCY BANDS FOR MONITORING FOREST REGIONS USING POLSAR SYSTEMS

A SAR operating at wavelengths ranging from a few centimeters to a few meters is more sensitive to larger canopy components [2]. The main scatterers in a canopy are the elements having dimensions of the order of the wavelength as shown in Figure 2. The leaves and small particles of the canopy are imaged in the X-band and C-band; the small branches are visible for a microwave in the C-band and L-band. At lower frequencies (e.g., P-band wavelength is 70 cm), the microwaves penetrate through leaves and small branches, and the scattering is mainly caused by large branches, trunks, and the ground surface. At VHF band, the tree trunks and soil surface are the main source of scattering.

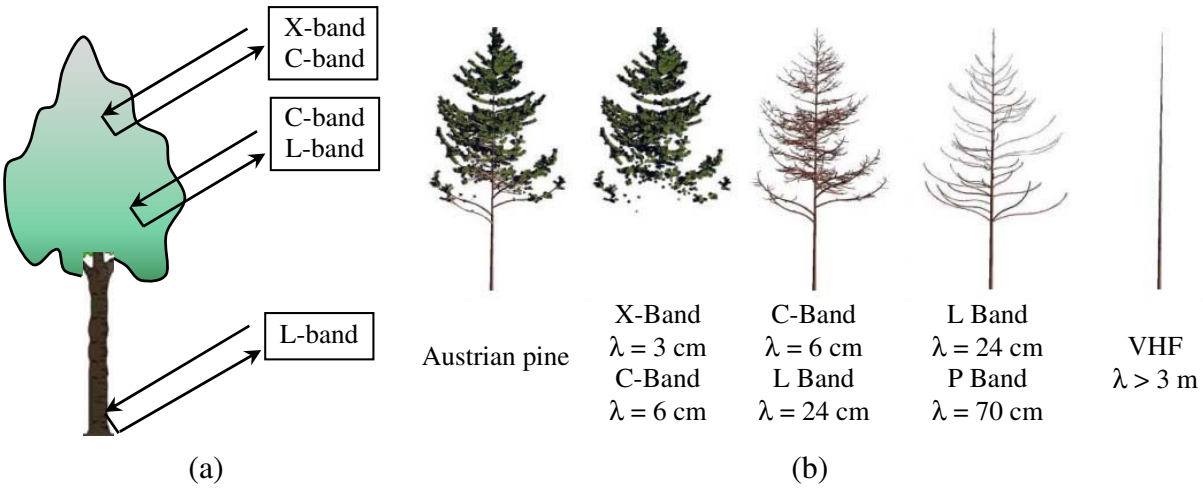

Figure 2. The dominant scatterers in a forest region for different frequency bands.

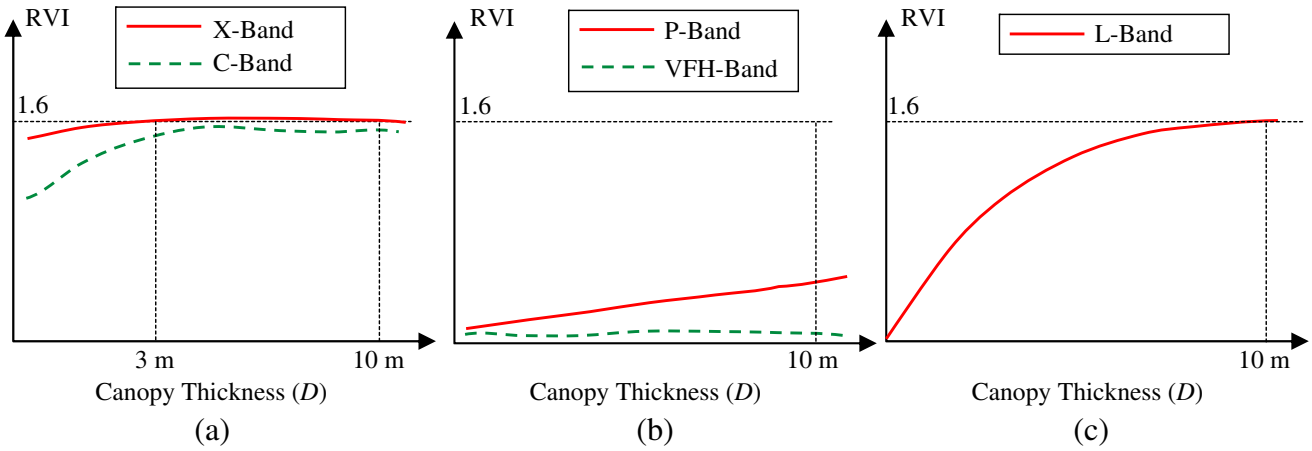

Figure 3. Variation of the RVI with the thickness of the canopy layer for different bands of the operating frequency.

Table 1. Expressions for the dependence of the RVI on the canopy layer thickness at the different frequency bands for the SAR operation.

Frequency	D-RVI Relation
VHF-Band (145 MHz)	$1.6\,(1 - e^{-0.005D})$
P-Band (450 MHz)	$1.6\,(1 - e^{-0.02D})$
L-Band (1.7 GHz)	$1.6\,(1 - e^{-0.5D})$
C-Band (5.0 GHz)	$1.6\,(1 - e^{-1.2D})$
X-Band (10.0 GHz)	$1.6\,(1 - \mathrm{e}^{-2.0D})$

Irrespective of the height of canopy layer top, the most appropriate band for accurate estimation of the forest vertical profiles for the forest regions with canopy layer thickness $D < 10\,\mathrm{m}$ is the L-band. Figure 3 shows the variation of the RVI with the canopy layer thickness for different bands of the operating frequency. Table 1 gives the corresponding (approximate) expressions. Such expressions have been obtained by electromagnetic simulation using plane wave incident on ensemble of random volume models above rough surface. Curve fitting is then applied to get such closed-form expressions. In X-band, the RVI seems constant at its maximum possible value (1.6) even for very thin canopy layer. In VHF-band, the RVI seems very low (< 0.1) and is almost independent of the canopy layer thickness. In C-band, the RVI has weak dependence on the canopy layer thickness for $D < 3\,\mathrm{m}$ and is almost independent of D for $D > 3\,\mathrm{m}$. In P-band, the RVI has very weak dependence on the canopy layer thickness for $D < 10\,\mathrm{m}$; however, it has stronger dependence for $D > 10\,\mathrm{m}$ and can be useful to estimate canopy layer thickness with a few dozens of meters. It is clear that the RVI is strongly dependent on the canopy thickness in for $0 < D < 10\,\mathrm{m}$; hence, the proposed method gives the best accuracy when being used to estimate the canopy thicknesses lying in this range.

4. COMPOSITION OF BACKSCATTERING FROM FOREST AREAS USING THE THREE-COMPONENT SCATTERING MODEL

As shown in Figure 4, the SAR scattering coefficients for forest areas can be considered as composed of five components.

(i) Volume scattering from the tree crowns without complete penetration through the canopy layer (S_V).

(ii) Surface scattering (single bounce) from bare ground surface (S_S).

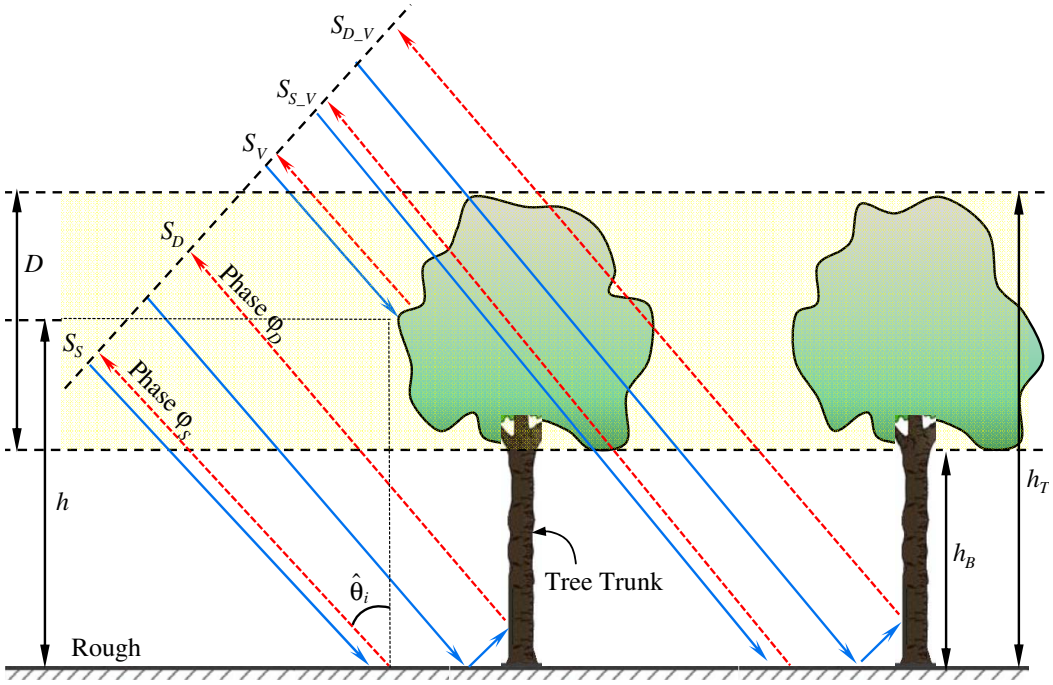

Figure 4. Components of the PolSAR coefficients of backscattering from forest areas due to different scattering mechanisms.

(iii) Corner scattering (double bounces) on the bare ground then on the tree trunks (S_D).

(iv) Scattering of a wave passing through the canopy layer (complete penetration) then making single bounce on the ground surface (S_{S_V}).

(v) Scattering of a wave passing through the canopy layer (complete penetration) then making double bounces on the corners formed by the ground surface and tree trunks (S_{D_V}).

Thus, in view of the geometry presented in Figure 4, the backscattering coefficient of a resolution cell that belongs to a forest region can be expressed as follows

$$S_{\text{Forest}} = \alpha S_V + \beta S_S e^{-j\varphi_S} + \gamma S_D e^{-j\varphi_D} + \eta S_{S\_V} e^{-j\varphi_S} + \zeta S_{D\_V} e^{-j\varphi_D} \tag{1}$$

where $|\alpha|^2$, $|\beta|^2$, $|\gamma|^2$, $|\eta|^2$, and $|\zeta|^2$ are positive real quantities related to the probabilities of the existing of the corresponding land cover constituents in the ground resolution cell under consideration. It is assumed that the incident power illuminates the forest area such that

$$|\alpha|^2 + |\beta|^2 + |\gamma|^2 + |\eta|^2 + |\zeta|^2 = 1 \tag{2}$$

The scattering coefficients S_{S_V} (or S_{D_V}) are caused by the rays that make single-bounce (or double-bounces). Those rays suffer passing through the canopy layer twice, during the incidence and another time after the reflection on the ground surface (or ground-trunk corners). These scattering coefficients can be expressed as follows.

$$S_{S\_V} = S_V^{(F)} S_S S_V^{(F)} = S_V^{(F)^2} S_S \tag{3}$$

$$S_{D_V} = S_V^{(F)} S_D S_V^{(F)} = S_V^{(F)^2} S_D \tag{4}$$

where $S_V^{(F)}$ is the volume scattering coefficient in the forward direction (i.e., the direction of the incident wave). Substituting from Eqs. (3) and (4) into Ew. (1), the following expression is obtained for backscattering coefficients of the forest areas.

$$S_{\text{Forest}} = \alpha S_V + \beta S_S e^{-j\varphi_S} + \gamma S_D e^{-j\varphi_D} + \eta S_V^{(F)^2} S_S e^{-j\varphi_S} + \zeta S_V^{(F)^2} S_D e^{-j\varphi_D} \tag{5}$$

where φ_S (or φ_D) is the phase difference between the rays backscattered from the ground surface (or ground-trunk corners) and those backscattered from the canopy layer without complete penetration through it. The path differences between the rays making single-bounce (or double-bounces) and those scattered completely from the canopy layer can be calculated with the aid of the geometry presented in Figure 4. Thus, the phase differences φ_{SB} and φ_{DB} can be expressed as follows.

$$\varphi_S = \frac{4\pi h}{\lambda \cos\hat{\theta}_i} \tag{6}$$

$$\varphi_D = \frac{4\pi h}{\lambda \cos\hat{\theta}_i} + \frac{\pi h}{\lambda \cos\hat{\theta}_i} = \frac{5\pi h}{\lambda \cos\hat{\theta}_i} \tag{7}$$

where h is the height of the canopy layer center above the ground surface.

$$h = \frac{1}{2}\left(h_T + h_B\right) = \frac{1}{\pi}\left(\varphi_D - \varphi_S\right)\ \lambda \cos\hat{\theta}_i \tag{8}$$

where h_T and h_B are the heights of the top and bottom of the canopy layer, respectively.

Equation (5) can be rearranged as follows.

$$S_{\text{Forest}} = \alpha S_V + \left(\beta + \eta S_V^{(F)^2}\right) e^{-j\varphi_S} S_S + \left(\gamma + \zeta S_V^{(F)^2}\right) e^{-j\varphi_D} S_D \tag{9}$$

The last expression can be written as follows.

$$S_{\text{Forest}} = a_V S_V + a_S S_S + a_D S_D \tag{10}$$

where the coefficients a_V, a_S, and a_D are in general, complex coefficients expressed as follows.

$$a_V = \alpha \tag{11}$$

$$a_S = \left(\beta + \eta S_V^{(F)^2}\right) e^{-j\varphi_{SB}} \tag{12}$$

$$a_D = \left(\gamma + \zeta S_V^{(F)^2}\right) e^{-j\varphi_{DB}} \tag{13}$$

As given by Eqs. (6) and (7), the phases φ_S, and φ_D appearing in Eqs. (12) and (13) are directly proportional to the height h of the canopy layer center. This is useful, as explained later, for the estimation of the heights h_B and h_T of the bottom and top of the canopy layer, respectively.

5. MODELING UNIT CELL OF THE CANOPY LAYER AS CLOUD OF RANDOMLY DISTRIBUTED STRAIGHT DIPOLES

For realistic simulation of the forest canopy layer, a number of n_w randomly oriented and distributed thin dipoles can be used to construct a cloud shape like three-dimensional prism whose base is a rectangle. The front and back side faces of the prism are parallelograms lying in the vertical plane (plane of incidence) whose vertical sides are parallel to the direction of propagation of the incident wave as shown in Figure 5(a). The left and right faces of the prism are rectangular in shape with their planes parallel to the direction of incidence. The prism height is equal to the canopy thickness, D, which is expressed as follows.

$$D = h_T - h_B \tag{14}$$

To get the volumetric density of the dipoles within the prism constant with varying the canopy thickness, D, the total number of dipoles in the cloud should be proportional to D, i.e., $n_w \propto D$. This cloud can be used as unit cell which can be repeated horizontally to construct the entire canopy layer as shown in Figure 5(b). The random dipoles have random lengths and orientations over the prism volume. The dipoles locations are distributed within the prism volume with a uniform probability distribution function.

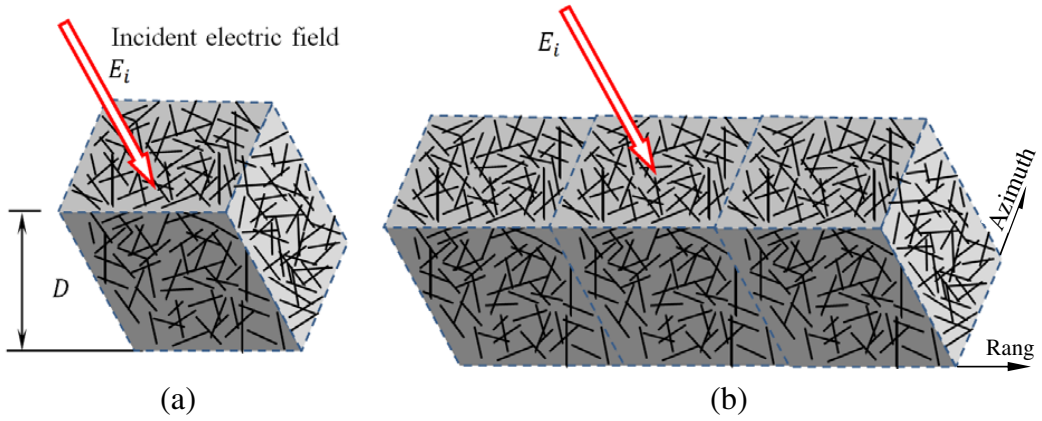

Figure 5. The geometrical model of a cloud of randomly oriented straight dipoles with uniform probability distribution function within the prism volume for building a model for the canopy layer. (a) Model for a unit cell of the dipoles cloud. (b) Multiple cells forming the entire canopy layer.

6. PROPOSED METHOD FOR ESTIMATION OF FOREST VERTICAL STRUCTURE USING THREE-COMPONENT SCATTERING MODEL

The proposed method depends on the estimation of the average height of the canopy layer central level, h, given by Eq. (8) and the average thickness of the canopy layer, D, given by Eq. (14). Using the estimated values of h and D, the average heights of the canopy layer top and bottom h_T and h_B, respectively, can be determined.

As previously mentioned, the inclined prism cloud of random straight dipoles described in detail in Section 5 is appropriate to model the canopy layer of the forest areas in which the tree canopies are overlapping. This model is employed in the present section to develop a method for estimating the forest vertical structure.

The elements of the covariance matrix of the PolSAR channels data can be used to evaluate the ensemble average of the RVI and the normalized RCS over a set of pixels in the multiple-channel PolSAR image.

The covariance matrix of PolSAR 3-channel data can be expressed as follows [20].

$$C = \begin{bmatrix} \sigma_{hh}^2 & \sqrt{2}\sigma_{hh,hv}^2 & \sigma_{hh,vv}^2 \\ \sqrt{2}\sigma_{hv,hh}^2 & 2\sigma_{hv}^2 & \sqrt{2}\sigma_{hv,vv}^2 \\ \sigma_{vv,hh}^2 & \sqrt{2}\sigma_{vv,hv}^2 & \sigma_{vv}^2 \end{bmatrix} \tag{15}$$

The ratio of the average backscattered power to the power illuminating the target (resolution cell) can be evaluated as the sum of the main diagonal elements of C. This ratio can be expressed as follows.

$$P = \sigma_{hh}^2 + 2\sigma_{hv}^2 + \sigma_{vv}^2 \tag{16}$$

The RVI is calculated from the elements of the covariance matrix of the PolSAR channels data collected for the forest region as follows [7].

$$\text{RVI} = \frac{8\sigma_{hv}^2}{\sigma_{hh}^2 + \sigma_{vv}^2 + 2\sigma_{hv}^2} \tag{17}$$

As the RCS of a target is defined as the ratio between the backscattered power, P_{BS}, and the incident power density, P_d [21], at the target location, it can be expressed as follows

$$\text{RCS} = \frac{P_{BS}}{P_d} \tag{18}$$

The normalized radar cross section, RCS_N, of an object is defined as the ratio between the RCS of this object and its (physical) cross-sectional area, A_T, in the transverse plane of the incident plane

wave. Thus it can be expressed as

$$\mathrm{RCS}_N = \frac{\mathrm{RCS}}{A_T} \tag{19}$$

Substituting for the RCS from Eq. (18) into Eq. (19), one gets

$$\mathrm{RCS}_N = \frac{P_{BS}}{P_d A_T} \tag{20}$$

The incident power illuminating the object, P_i, can be expressed as

$$P_i = P_d A_T \tag{21}$$

Making use of Eq. (21), the expression (20) for the normalized RCS can be expressed as

$$\mathrm{RCS}_N = \frac{P_{BS}}{P_i} \tag{22}$$

Thus, the normalized RCS of a target can be simply defined as the ratio of the backscattered power relative to the power illuminating the target. This ratio is expressed in Eq. (16) in terms of the covariance matrix elements.

$$\mathrm{RCS}_N = \sigma_{hh}^2 + \sigma_{vv}^2 + 2\sigma_{hv}^2 \tag{23}$$

6.1. Estimation of the Canopy Layer Thickness and Soil Surface Roughness

Increasing the thickness of the forest canopy layer causes higher level of backscattered power due to the increase of the number of random dipoles in the direction of incidence of the plane wave. Accordingly, it is expected that the RCS of a forest area increases with increasing the thickness of the canopy layer. It is also expected that, for a specific frequency, the rate of increase of the RCS with increasing the canopy layer thickness will decay until it saturates when the thickness reaches a value after which the microwave signal can no more penetrate into the canopy. Of course, the decay rate depends on the frequency of the microwave signal such that the higher the microwave frequency is, the faster the rate of decay of the RCS is. A microwave of lower frequency can penetrate thicker canopy layer, and hence, the frequency required to estimate the canopy layer should be low enough to pass through the entire canopy layer.

On the other hand, if the operating frequency is too high for the microwave to fully penetrate the entire canopy layer, it is expected that the RVI will have an almost constant value that can closely change near its maximum value (about 1.6) irrespective of the canopy layer thickness. If the operating frequency allows the complete penetration through the canopy layer, the backscattering due to the double-bounces on the corners constructed by the ground/tree-trunks will significantly decrease the RVI calculated from the total backscattering due to the entire forest structure.

The other factors affecting the dependence of both the RCS and RVI of the forest areas are the roughness degree of the ground surface. The lower the ground roughness is, the higher the backscattering caused by the double-bounces is. As already known, the backscattering due to single- and double-bounces has a very low level of cross polarization, and hence, the RVI of bare ground surface or ground/tree-trunks corners is near zero. Consequently, as the contribution of the backscattered power due to double-bounces becomes higher the total RVI of the forest area becomes lower.

The relation between RCS and the canopy layer thickness D for given values of the ground roughness R_G and wall roughness R_W can be obtained by fitting an exponential function to the D-RCS data obtained by electromagnetic simulation together with the three-component scattering model as described above. On the other hand, the relation between RVI and the canopy thickness, D, can be obtained by fitting an exponential function using the D-RVI data obtained by simulation. It is assumed that the roughness of the tree trunk surface, R_W, is relatively low in comparison to the ground roughness and can be assigned the same value for all the trees, which is practically convenient for the majority of the forest areas.

6.1.1. Fitted D-RCS Relation for Constant R_G

As discussed before, it is expected that with increasing the canopy thickness, the RCS of the (composite) forest structure, as measured by the PolSAR, approaches an asymptotic value. Considering this behavior, the most suitable fit relation between the RCS and canopy thickness is an exponential relation that takes the following form.

$$\mathrm{RCS} = a_1 - a_2 e^{-a_3 D} \tag{24}$$

In this relation, a_1, a_2, and a_3 should be real positive.

It can be shown that the inverse relation that describes the canopy layer thickness as a function of the RCS can be expressed as follows.

$$D = b_1 \ln\left(b_2 \mathrm{RCS} + b_3\right) \tag{25}$$

where,

$$b_1 = \frac{1}{-a_3}, \quad b_2 = \frac{1}{-a_2}, \quad b_3 = \frac{a_1}{a_2} \tag{26}$$

Obviously, b_1 and b_2 are negative, whereas b_3 is positive to realize the correct behavior. The coefficients a_1, a_2, and a_3, or alternatively, b_1, b_2, and b_3 can be determined for a specific value of the ground roughness R_G using an appropriate curve fitting technique.

6.1.2. Fitted D-RVI Relation for Constant R_G

The behavior of the measured RVI with increasing the canopy layer thickness is similar to that of the normalized RCS. Consequently, in a way similar to that described in Section 6.1.1, a mathematical relation can be fitted for the canopy layer thickness as a function of RVI. Thus, the following expression can define such a relationship.

$$D = c_1 \ln\left(c_2 \mathrm{RVI} + c_3\right) \tag{27}$$

The coefficients c_1 and c_2 should be negative, whereas c_3 should be positive to satisfy the correct RVI dependence on the canopy layer thickness.

Upon the knowledge of the normalized RCS and the RVI from the measured PolSAR data for a given region of the forest, the relations given by Eqs. (25) and (27) can be used to uniquely identify the canopy layer thickness.

6.1.3. Fitted D-R_G Relation for Constant Normalized RCS

It can be shown that, to get constant RCS of forest regions with varying canopy layer thickness, D_{RCS}, and ground roughness, $R_{G_{\mathrm{RCS}}}$, the relation between the latter two parameters should be quadratic as follows.

$$D_{\mathrm{RCS}} = d_2 R_{G_{\mathrm{RCS}}}^2 + d_1 R_{G_{\mathrm{RCS}}} + d_0 \tag{28}$$

where d_0, d_1, and d_2 are constants to be determined.

6.1.4. Fitted D-R_D^G Relation for Constant RVI

It can be shown that, to get the constant RVI of forest regions while varying canopy layer thickness, D_{RVI}, and ground roughness, $R_{G_{\mathrm{RVI}}}$, the relation between the latter two parameters should be quadratic as follows.

$$D_{\mathrm{RVI}} = e_2 R_{G_{\mathrm{RVI}}}^2 + e_1 R_{G_{\mathrm{RVI}}} + e_0 \tag{29}$$

where e_0, e_1, and e_2 are constants to be determined.

Equations (28) and (29) are actually obtained as fitted relations by generating numerical data using the relations in Eqs. (25) and (27). As the canopy layer thickness, D, and ground roughness, R_G, are two main parameters which are not known during the collection of the PolSAR data, the proposed method should evaluate them together. For the specific values of the RCS and RVI measured by the PolSAR system, Equations (28) and (29) are solved together to get the unknown canopy layer thickness and ground roughness.

6.2. Estimation of the Canopy Layer Height

The unknown complex coefficients a_S and a_D can be evaluated by solving Equation (10) using the collected coherent PolSAR data for the ground resolution cells of the imaged forest region. The phase difference between a_S and a_D can be obtained to get the height of the canopy layer center, h, relative to the average heights of the points on the soil surface using Eq. (8). Upon the knowledge of the estimated value of D using the method described in Section 6.2, Equations (8) and (14) an be solved together to get the heights of the bottom and top of the canopy layer, h_B and h_T, respectively.

7. RESULTS AND DISCUSSIONS

It should be noted in the following presentations and discussions of the simulation results that the wall (tree trunk surface) roughness, R_W, is set to 0.025, which is a practical value for most of the natural trees. Also, it should be noted that the rough surface of the ground soil is assumed to be Gaussian with isotropic statistical properties and has a correlation length of 0.47 m, which is a typical value for the soil surface roughness in most of the forest regions. During electromagnetic simulation, it is assumed that the direction of propagation of the incident plane wave makes an angle of 45° with the gravity direction and that the operating frequency is 1.27 GHz. It is assumed that the tree trunk has dielectric constant $\varepsilon_{r_w} = 4$ and electric conductivity $\sigma_w = 1\,\mathrm{S/m}$. Also, it is assumed that the forest regions under investigation have clayey soil with dielectric constant $\varepsilon_{r_g} = 4$ and conductivity $\sigma_g = 1\,\mathrm{S/m}$. The canopy layer thickness and the roughness of the soil surface are unknown and required to be determined.

7.1. Characteristics of Backscattering from Forest Canopy in the Absence of Single- and Double-Bounces

A unit cell of the canopy layer is modeled as a cloud of randomly oriented thin straight dipoles. The cloud has its three-dimensional shape as parallelogram prism as described in Section 5. For this model, in the absence of the contribution of single- and double-bounces, the backscattering coefficient can be reduced as follows

$$S_{\mathrm{Forest}} = S_V \tag{30}$$

which is obtained by setting $\alpha = 1$, $\beta = 0$, $\gamma = 0$, $\eta = 0$, and $\zeta = 0$ in Eq. (5) or (9).

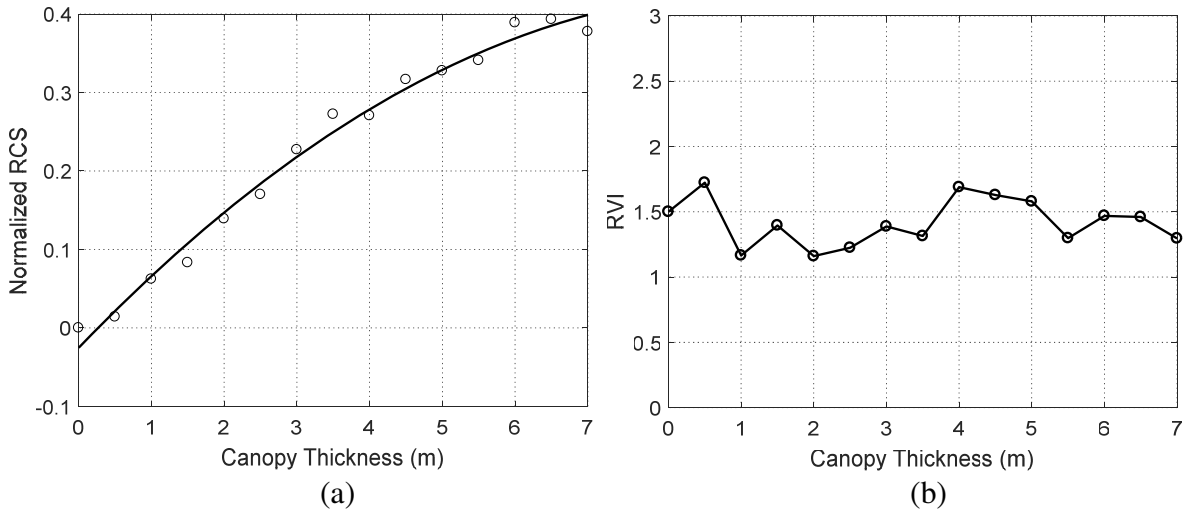

Figure 6. Dependence of the normalized RCS and RVI on the canopy height due to a plane wave incident in the direction making 45° with the normal to the ground in the absence of single- and double-bounces. (a) Dependence of the RCS on the canopy thickness. (b) Dependence of the RVI on the canopy thickness.

10 cloud samples are generated as described in Section 5 for each of the following canopy thicknesses 0.5, 1.0, 1.5, 2.0, 2.5, 3.0, 3.5, 4.0, 4.5, 5.0, 5.5, 6.0, 6.5, and 7.0 m. Thus, for each thickness there is an ensemble of size 10 samples. The results of the RVI and normalized RCS corresponding to each canopy thickness are averaged over each ensemble.

Figure 6 shows the dependence of the ensemble-averaged RCS and RVI on the thickness of the canopy layer. The results are obtained by EM simulation due to a plane wave incident (in the direction making 45° with the normal to the ground) on a unit cell of the canopy model like that described above. As shown in Figure 6(a), the RCS increases with increasing the canopy thickness. On the other hand, the RVI, Figure 6(b), is closely varying around almost constant value ranging from 1.2 to 1.7 irrespective of the canopy layer thickness. This behavior is similar to that of the RVI data collected by practical SAR systems [12, 13] for natural vegetation areas with very dense vegetation canopies.

7.2. Characteristics of Backscattering due to Single-Bounce on the Rough Surface of the Soil

The normalized RCS due to a plane wave obliquely incident on the ground surface (suffering a single-bounce) is strongly dependent on the surface roughness. An ensemble of 30 samples of rough surface models with the same statistical parameters is created. The normalized RCS and RVI are evaluated through a Monte-Carlo method by carrying out EM simulation to calculate these radar quantities for each sample and then carrying ensemble averaging for the obtained results. As shown in Figure 7(a), the ensemble-averaged normalized RCS due to a plane wave incident in the direction making 45° with the gravity is plotted against the ground roughness. As shown in the figure, the RCS increases with increasing the surface roughness.

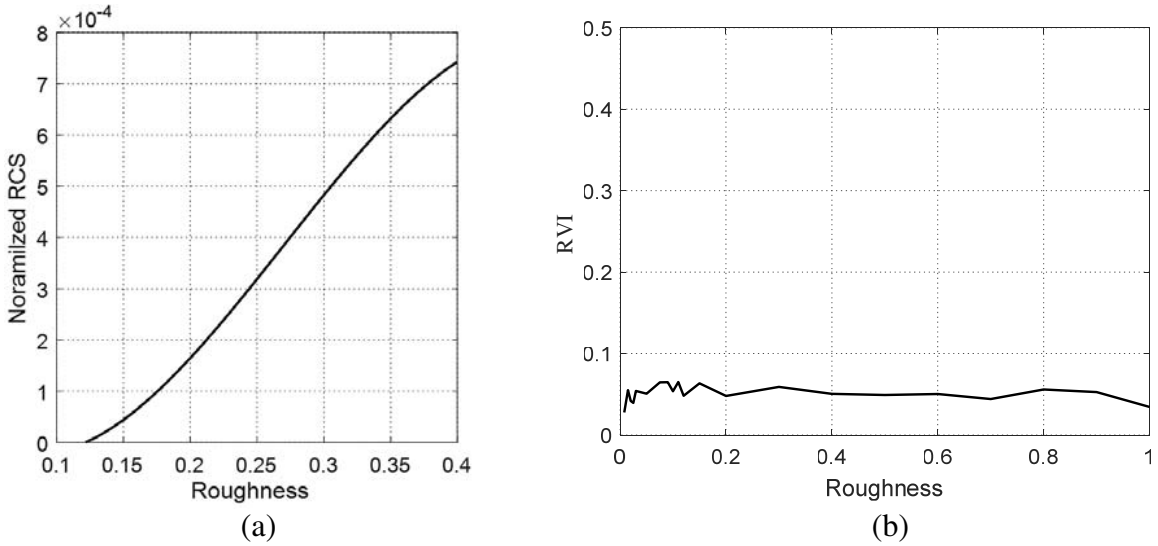

Figure 7. Dependence of the normalized RCS and the RVI on the ground roughness due to a plane wave incident in the direction making 45° with the normal to the ground. (a) Dependence of the RCS on the ground surface roughness. (b) Dependence of the RVI on the ground surface roughness.

On the other hand, the RVI calculated from the backscattering data due to single-bounce of the plane waves on such a surface is presented in Figure 7(b) against the surface roughness. As shown in this figure, the RVI is very low as the isotropic rough surface does not cause significant cross polarization of the backscattered waves under the assumption of single-bounce scattering. Also, it is shown that the RVI is almost independent of the ground roughness under the assumption of isotropic statistical properties.

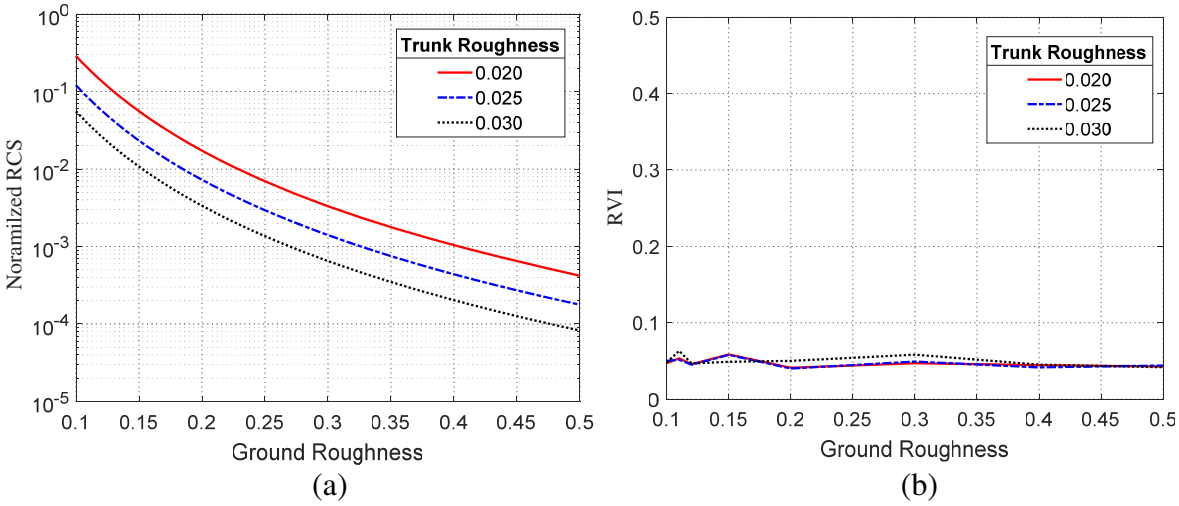

Figure 8. Dependence of the normalized RCS and the RVI on the ground roughness for different values of the trunk surface roughness due to a plane wave incident in the direction making 45° with the normal to the ground. (a) Dependence of the RCS on the ground and trunk roughness degrees. (b) Dependence of the RVI on the ground and trunk roughness degrees.

7.3. Characteristics of Backscattering due to Double-Bounces on the Ground-Trunk Corners

The averaged normalized RCS due to the double-bounces on the corners formed by the horizontal ground surface and the vertical tree trunks is strongly dependent on the roughness degrees of the ground surface as well as the trunk surface roughness. As shown in Figure 8(a), the normalized RCS sharply decays with increasing the surface roughness of both the ground (R_G) and the trunk (R_W).

The RVI calculated from the coefficients of backscattering due to double-bounces of the plane waves on the ground-trunk corners is presented in Figure 8(b) against the roughness degree of the ground surface, R_G, for different values of the roughness degree of the wall (trunk), R_W. As shown in this figure, the RVI is very low as the isotropic rough surfaces of both the ground and the tree trunks do not cause significant cross polarization of the backscattered waves. Also, it is shown that the RVI is almost independent of the roughness of the ground and wall surfaces under the assumption of isotropic statistical properties of both surfaces.

7.4. Characteristics of Backscattering Parameters for the Entire Forest Structure

As discussed in Section 4, the backscattering coefficients for natural forest areas usually have contributions of single- and double-bounces in addition to the volume scattering from the canopy layer. Assuming that only the three parameters α, β and γ are non-zero, the basic three-component scattering model of the forest area can be expressed as follows.

$$S_{\text{Forest}} = \frac{1}{\sqrt{3}} \left(S_V + S_S e^{-j\varphi_S} + S_D e^{-j\varphi_D} \right) \tag{31}$$

which is obtained from Eq. (10), by setting $a_V = \frac{1}{\sqrt{3}}$, $a_S = \frac{1}{\sqrt{3}} e^{-j\varphi_S}$, $a_D = \frac{1}{\sqrt{3}} e^{-j\varphi_D}$, with $\eta = 0$, and $\zeta = 0$.

To simulate backscattering from a forest area composed of the three constituents whose RCS and RVI are those obtained by simulation as described in the last three Sections 7.1, 7.2, and 7.3, expression (31) is used to get S_{Forest} with the backscattering coefficients S_V, S_{SB}, and S_{DB} obtained for the same constituents through EM simulation.

The dependencies of the RCS and RVI on the canopy layer thickness due to a plane wave incident in the direction making 45° with the normal to the ground are presented in Figure 9 for trunk roughness of 0.025 and different values of the ground roughness.

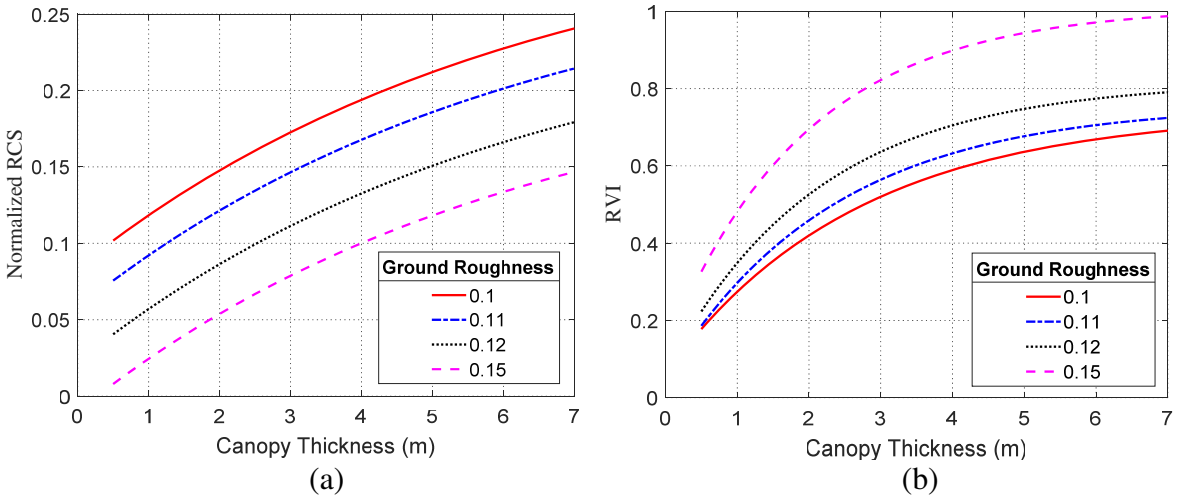

Figure 9. Dependence of the RCS and RVI on the canopy layer thickness using the three-component scattering model given by (31) for trunk roughness of 0.025.

It is shown, in Figure 9(a) that, for specific values of the ground and trunk surface roughness, the RCS of such composite forest area increases with increasing the thickness of the canopy layer. It is also shown that, under the operating frequency (1.27 GHz), the rate of increase of the RCS decays with a tendency to saturate when the thickness reaches a specific value after which the plane wave can no more pass through (fully penetrate) the canopy layer to impinge on the underlying ground surface and tree trunks.

On the other hand, the RVI increases with increasing the canopy height as shown in Figure 9(b). Like the behavior of the RCS with increasing the canopy thickness as described above, the rate of increase of the RVI decays until it saturates when the thickness reaches a specific value. This can be physically interpreted as follows. As the canopy thickness increases, the backscattered power from the canopy layer increases, see Figure 6(a), whereas the backscattered power from the ground-trunk corners (double-bounces) remains constant as it is independent of the canopy. Thus, with increasing the canopy layer thickness, the total SAR scattering coefficients have more contribution of the backscattering from the canopy layer and lower contribution of the backscattering from the double-bounces. Consequently, the RVI increases with increasing the canopy layer thickness. After the canopy layer thickness reaches a high enough value, the plane wave can no more pass through the canopy layer to impinge on the underlying ground surface and tree trunks. For such high values of the canopy layer thickness, the RVI is dominated by the contribution of the backscattering from the canopy layer. The RVI of the canopy layer is high and characterized by its independence of the canopy layer thickness as shown in Figure 6(b). The net effect is that the RVI of the composite structure saturates for large values of the canopy thickness as shown in Figure 9(b).

In summary, it has been shown that increasing the ground roughness has the effect of decreasing the backscattering (RCS) caused by the double-bounces. Hence, with increasing the ground roughness, the total RCS (of the composite structure) decreases whereas the RVI increases due to the increased contribution of the canopy layer to the total backscattering coefficients.

The curves presented in Figure 9 to describe the dependencies of the RCS and RVI on the canopy layer thickness can be used (in the inverse problem) to estimate the canopy layer thickness. The RCS and RVI can be calculated from the data collected by the PolSAR system; this is presented and discussed in detail in the following section.

7.5. Estimation of Canopy Layer Thickness and Ground Roughness for Forest Regions

In this section, the method described in Section 6.1 is applied to estimate the canopy layer thickness for a forest region with the default parameters and operating conditions given at the beginning of Section 7.

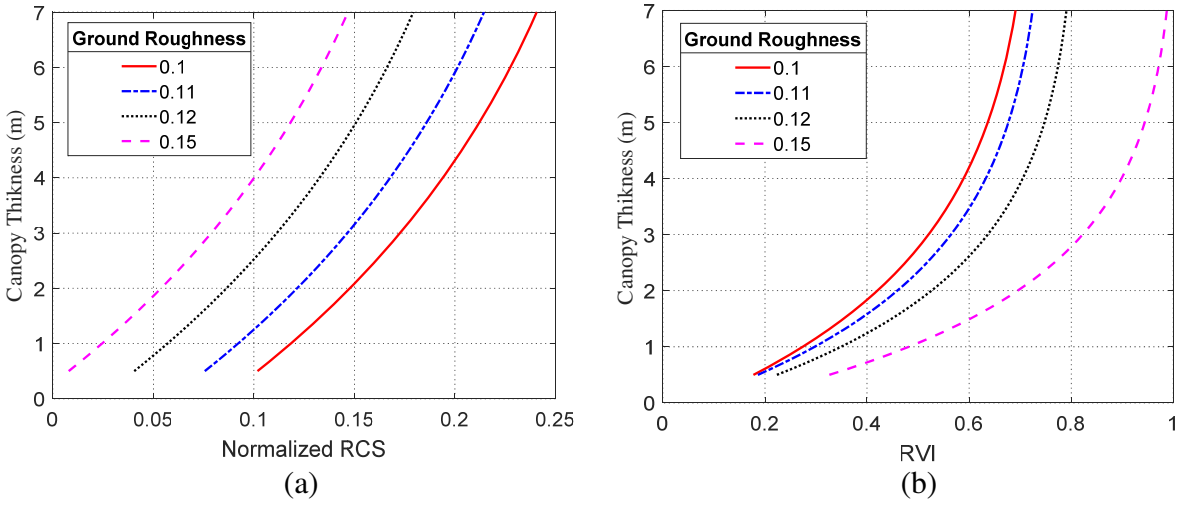

Figure 10. Fitted curves obtained for the dependence of the canopy layer thickness on both RCS and RVI for different values of the ground roughness R_G given that the trunk surface roughness $R_W = 0.025$.

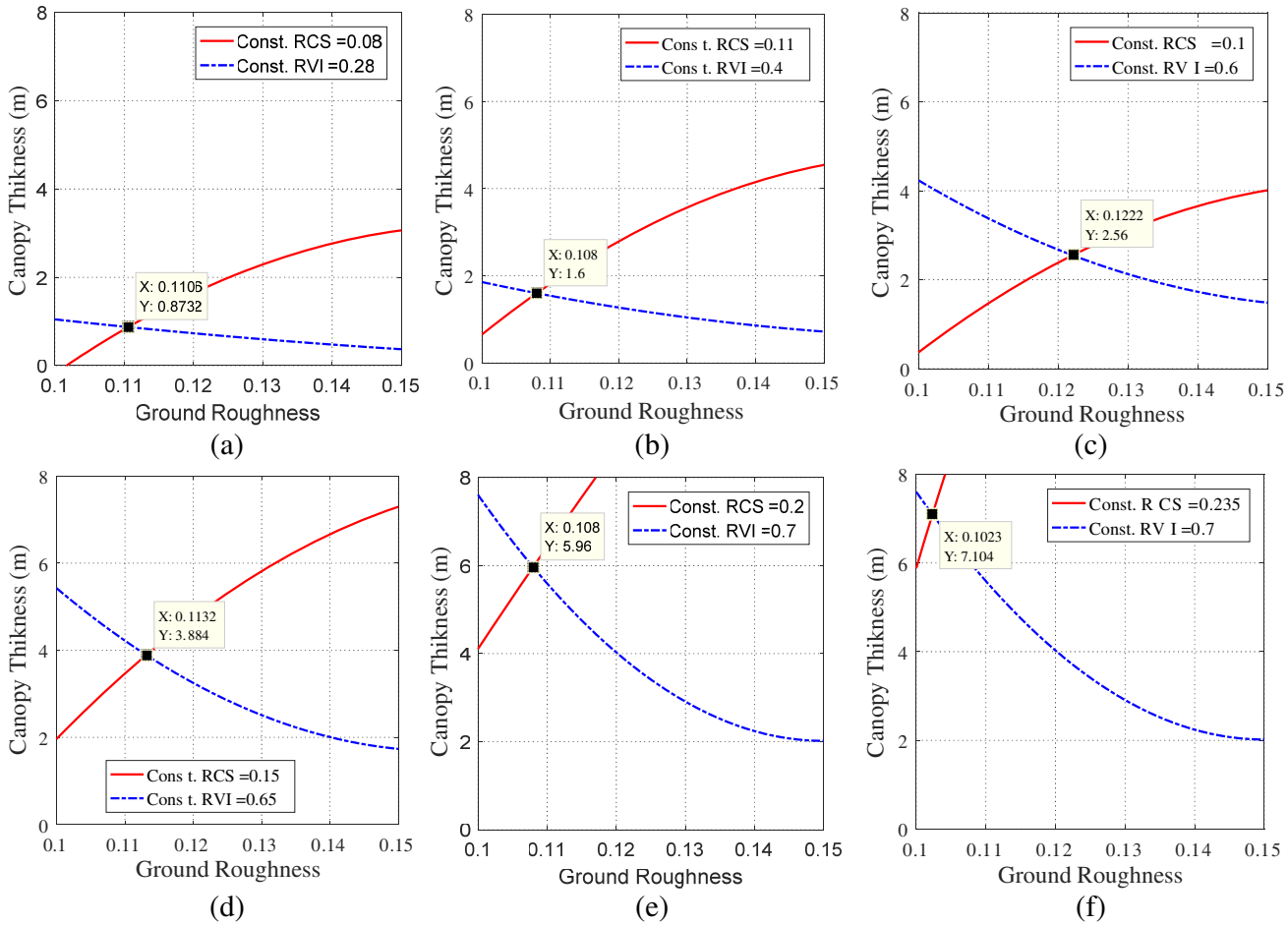

Figure 11. Graphical calculation of the estimated canopy thickness using the RCS and RVI calculate from simulated PolSAR data and the fitted relations (28) and (29).

The fitted curves obtained for the dependence of the canopy layer thickness on both RCS and RVI, expressed in Eqs. (25) and (27), are presented in Figures 10(a) and 10(b), respectively.

Some examples for applying the method described in Section 6.1 to estimate the canopy layer thickness are presented in Figure 11. For example, if the measured PolSAR data give normalized RCS = 0.15 and RVI = 0.65, the curves given by Eqs. (28) and (29) are plotted as shown in Figure 11(d) to be solved graphically. The point of intersection shows that the canopy layer thickness is about 3.88 m, and the ground roughness is about 0.113.

7.6. Examples for Estimation of Forest Vertical Structure

In this section, some examples are presented to demonstrate the capability of the method proposed in Section 6 for the estimation of the canopy thickness in forest regions using the four- or three-

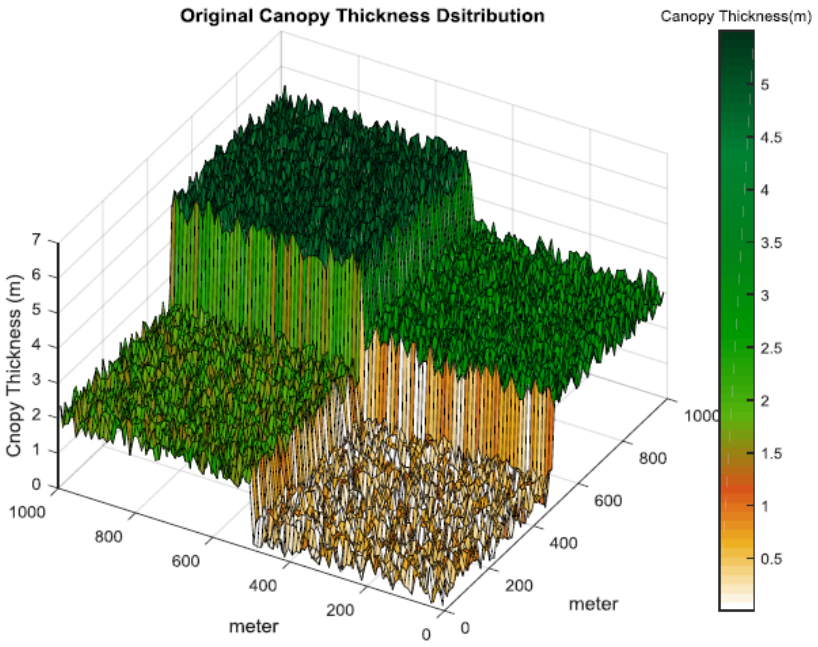

Figure 12. Ground truth for canopy thickness distribution for a geometrical model of a forest including four contiguous equal-area regions of canopy thicknesses 0.5, 2.0, 3.0, and 5.0 m.

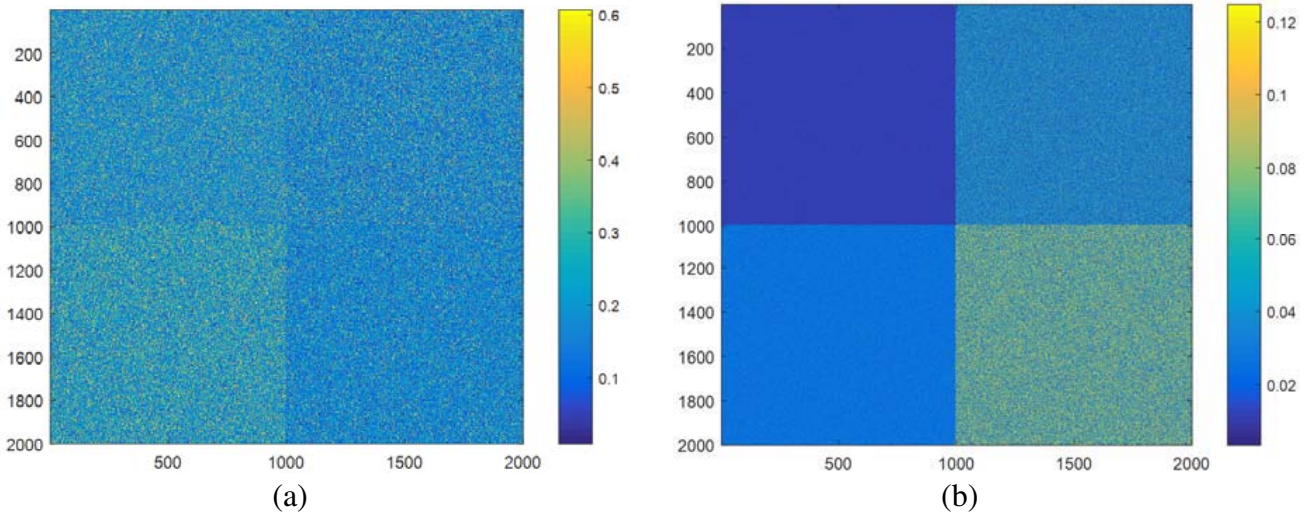

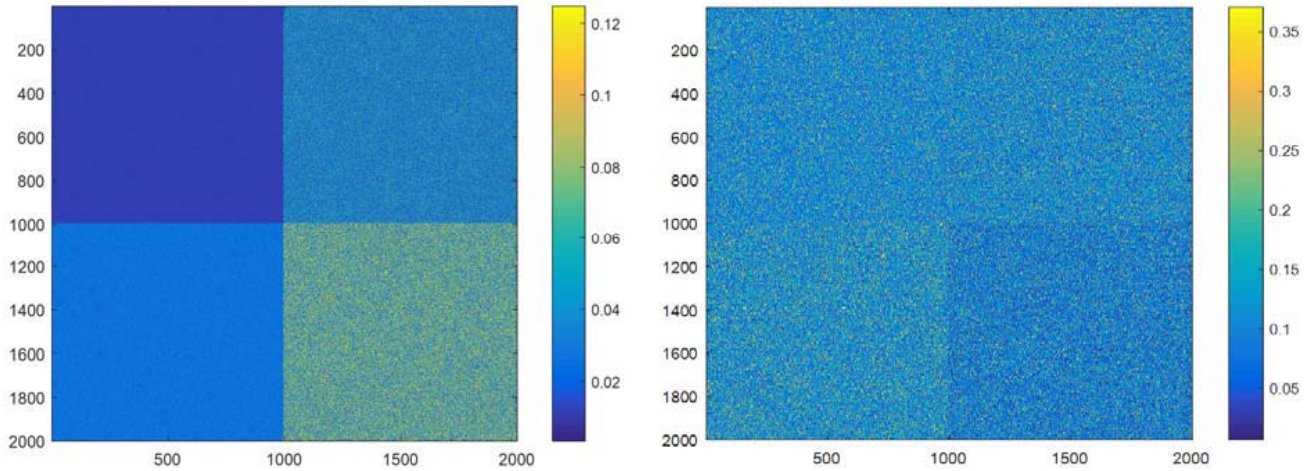

Figure 13. Visualized four-channel PolSAR data (images) for simulated forest (2000 × 2000 pixels) including four contiguous equal-area regions of canopy thicknesses 0.5, 2.0, 3.0, and 5.0 m, (a) $|S_{hh}|$, (b) $|S_{vh}|$, (c) $|S_{hv}|$, (d) $|S_{vv}|$.

channel PolSAR image. Figure 12 shows a three-dimensional graph for the ground truth of canopy thickness distribution for a geometrical model created for a (1000 m × 1000 m) forest region including four contiguous equal-area regions of canopy layer thicknesses 0.5, 2.0, 3.0, and 5.0 m. The four-channel PolSAR images obtained through EM simulation by applying the SAR target composition method described in Section 4 are presented in Figure 13 using SAR imaging resolution of 0.5 m × 0.5 m (image size 2000 × 2000 pixels). Each image is divided into 100 × 100 square cells, where each cell has 20 × 20 pixels. The corresponding distributions of the RVI (calculated for the group of pixels in each cell) and the normalized RCS (averaged over the pixels of each cell) are presented in Figures 14(a) and 14(b), respectively. Finally, the method described in Section 6 is applied to estimate the canopy thickness distribution over the imaged forest region. The estimated canopy thickness distribution is presented in

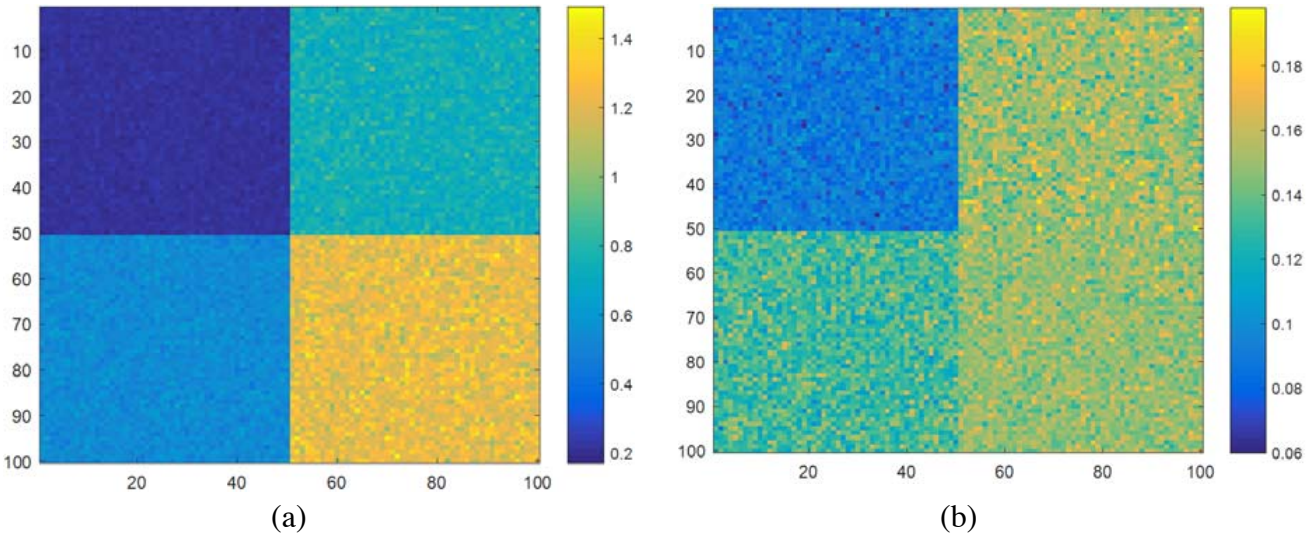

Figure 14. Distribution of the cell-averaged RVI and normalized RCS calculated for 100 × 100 cells (each of size 20 × 20 pixels) for the simulated forest regions whose PolSAR images are presented in Figure 13, (a) RVI, (b) normalized RCS.

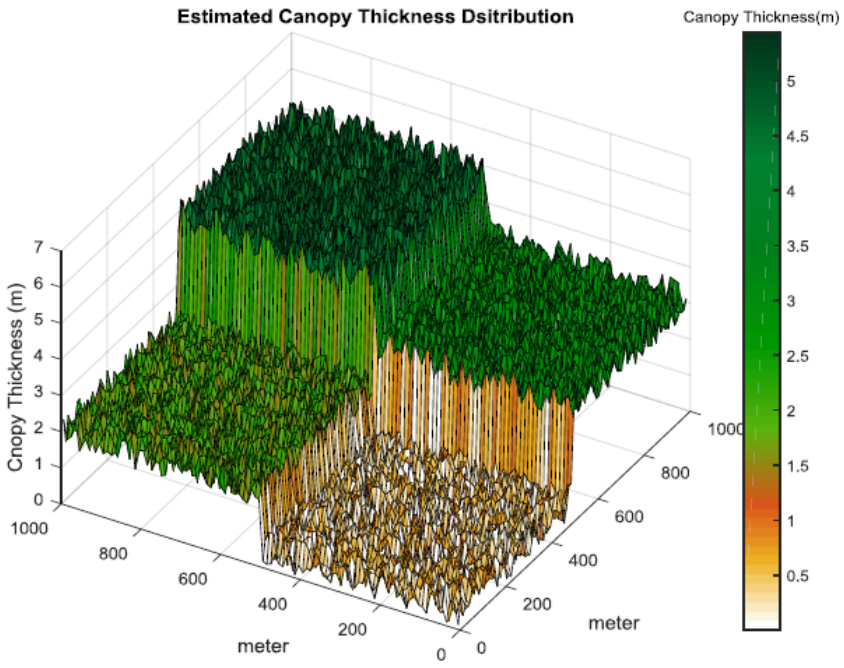

Figure 15. Estimated canopy thickness distribution for the geometric model of the four forest regions whose ground truth is presented in Figure 12.

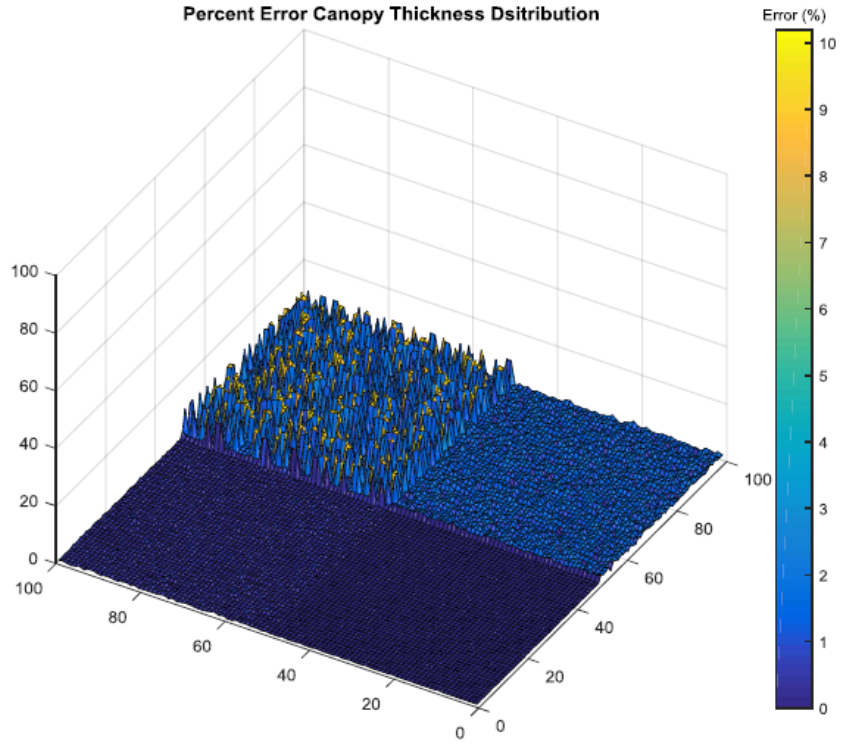

Figure 16. Percentage errors of the estimated canopy thickness distribution presented in Figure 15 whose ground truth is presented in Figure 12.

Figure 15. Comparing the estimated canopy thickness with the ground truth presented in Figure 12, the percentage error in the canopy thickness estimation for each cell of the forest area is obtained and presented in Figure 16. As shown in this figure, the maximum error in canopy thickness estimation is almost zero % for the forest region of the lowest thickness (0.5 m), negligible (< 2%) for the region of canopy thickness 2.0 m, very low (< 4%) for the region of canopy thickness 3.0 m, and acceptable (< 10%) for the region of the highest thickness (5.0 m). Such low values of the percentage error reflect the accuracy and efficiency of the method proposed in the present work for the estimation of the forest canopy layer thickness.

7.7. Estimation of Forest Vertical Structure

Other simulated PolSAR images similar to that presented in Figure 13 are generated for two contiguous forest regions with different canopy thicknesses and different heights of the canopy layer bottom h_B. The ground truth for the vertical structures of the two forest regions is presented in Figure 17. For the forest stand ranging from 0 to 500 m, the bottom height and thickness of the canopy layer are 5 m and 2.5 m, respectively. For the forest stand ranging from 501 to 1000 m, the bottom height and thickness of the canopy layer are 8.5 m and 5 m, respectively. The ground surface roughness is set to 0.11 for the two regions. The method described in Section 6 is applied to estimate the entire vertical structure of the two forest regions.

The estimated vertical structure is presented in Figure 17(b). Compared with the ground truth

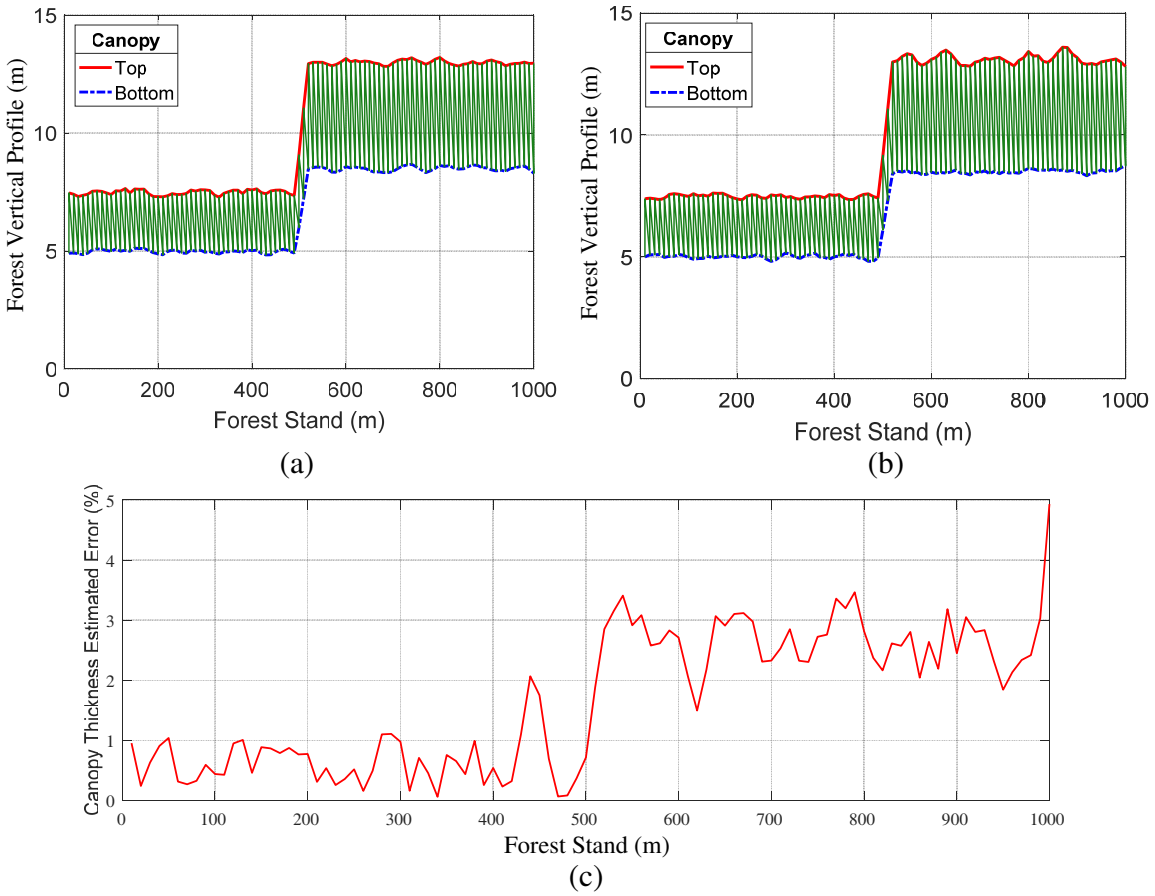

Figure 17. Estimated canopy thickness for two contiguous forest regions; the height of the canopy layer bottom is 5 m for the forest stand 0–500 m; the height of the canopy layer bottom is 8.5 m for the forest stand 500–1000 m; (a) Actual vertical profile (ground truth), (b) estimated vertical profile, (c) percentage error in the estimated canopy thickness.

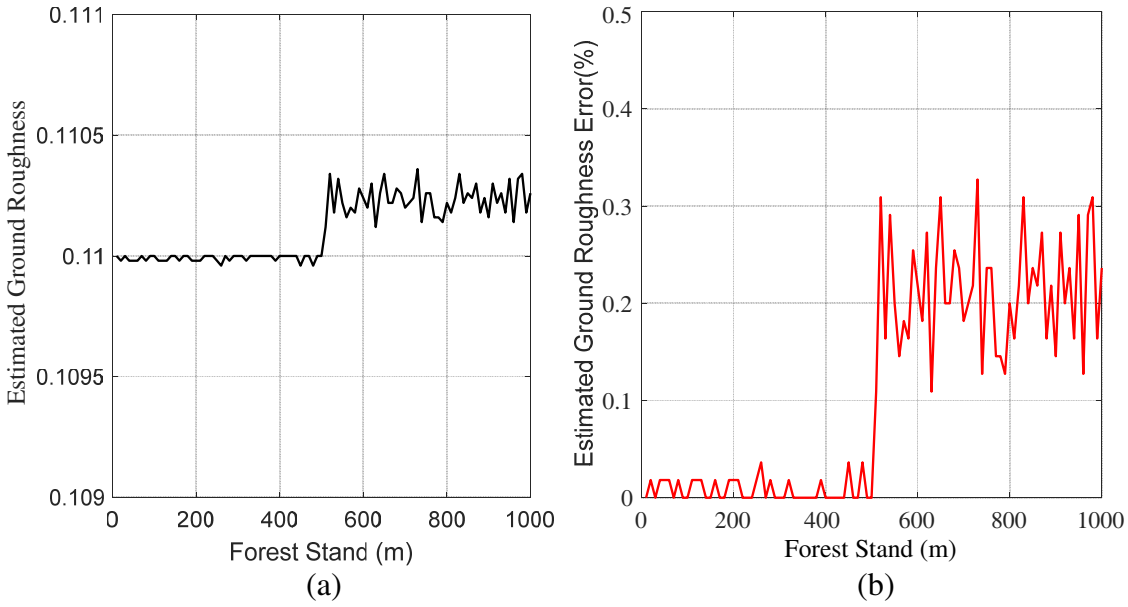

Figure 18. Estimated roughness of the ground for the two contiguous forest regions mentioned in Figure 17; the ground truth of the ground roughness is $R_g = 0.11$; (a) Estimated ground roughness, (b) percentage error in the estimated ground roughness.

presented in Figure 17(a), the vertical profile seems to be recovered with good accuracy. As the most important parameter of the vertical structure is the canopy layer thickness, Figure 17(c) presents the percentage error of its estimated value with the forest stand. As shown in the figure, the percent error does not exceed 2% for the forest region with canopy thickness 2.5 m and height 7.5 m, whereas it does not exceed 4% for the forest region with canopy thickness 5.0 m and height 13.5 m. Such high accuracy of canopy thickness estimation even for thin canopies reflects the efficiency of the proposed method.

On the other hand, the estimated roughness degree of the soil surface versus the forest stand is presented in Figure 18(a), and the corresponding percentage error is presented in Figure 18(b). The estimated roughness degree seems exact compared to the ground truth value (0.11) as the estimation error is very small or even negligible. For the forest stand ranging from 0 m to 500 m (canopy thickness = 2.5 m), the percentage error in the estimated roughness is negligible (almost zero). For the forest stand ranging from 500 m to 1000 m (canopy thickness = 5 m), the percentage error in the estimated roughness degree reaches about 0.3%. One can conclude that, for thicker canopy layers, not

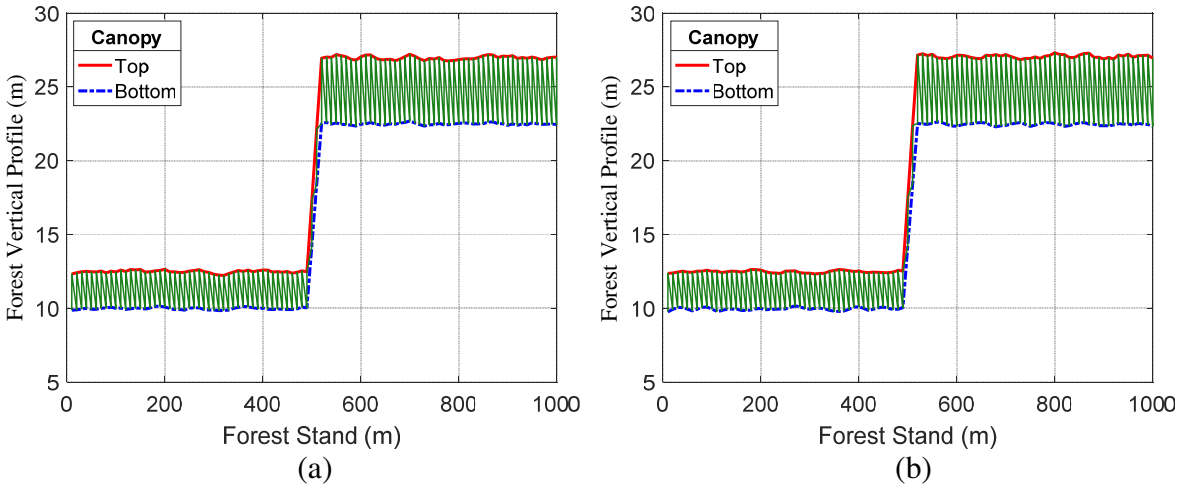

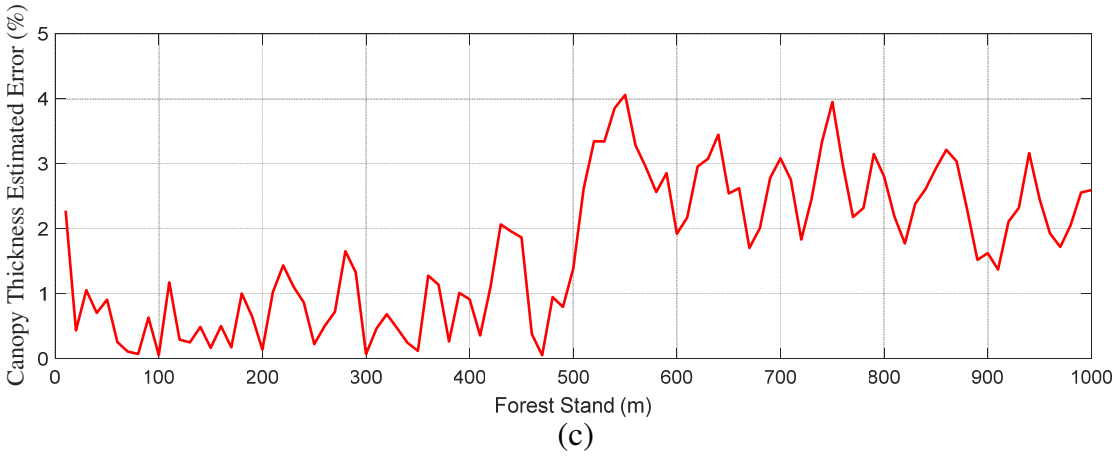

Figure 19. Estimated canopy thickness for two contiguous forest regions; the height of the canopy layer bottom is 10 m for the forest stand 0–500 m; the height of the canopy layer bottom is 22.5 m for the forest stand 500–1000 m; (a) Actual vertical profile (ground truth), (b) estimated vertical profile, (c) percentage error in the estimated canopy thickness.

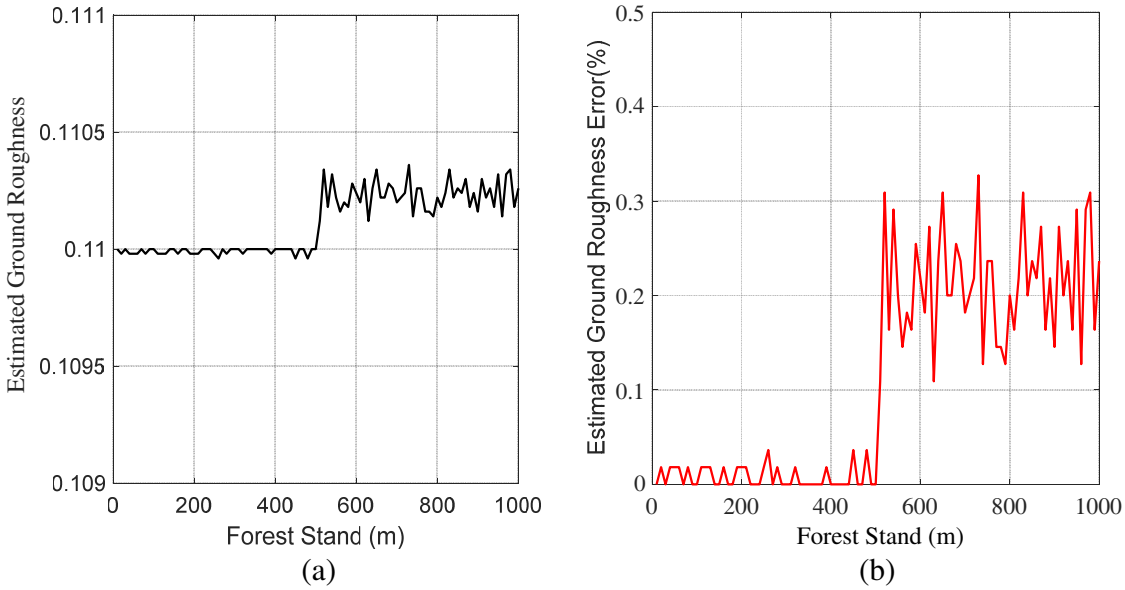

Figure 20. Estimated roughness of the ground for the two contiguous forest regions mentioned in Figure 19; the ground truth of the ground roughness is $R_g = 0.11$; (a) Estimated ground roughness, (b) percentage error in the estimated ground roughness.

only the error in estimated canopy thickness is larger than that for thinner canopies, but also the error in the estimated soil surface roughness is larger. However the resulting errors lie within acceptable limits.

To demonstrate the effect of the forest height on the accuracy of the proposed method PolSAR data are generated through simulation for two contiguous forest regions similar to those investigated in the previous example and having the same values of the canopy layer thicknesses but with much higher top. The average heights of the canopy layer top for the first and second forest regions are 12.5 m and 27.5 m, respectively. The ground truth of the forest vertical structure is presented in Figure 19(a). The same procedure is applied to get the estimated vertical structure which is presented in Figure 19(b). The percentage error of the estimated canopy layer thickness is presented in Figure 19(c). The resulting

error is almost like that of the previous example; the percent error does not exceed 2% for the forest region with canopy thickness 2.5 m and height 12.5 m, whereas it does not exceed 4% for the forest region with canopy thickness 5.0 m and height 27.5 m. Thus, one can conclude that the accuracy of the method proposed in the present paper to estimate the vertical structure of the forest seems independent of the forest height.

The estimated roughness degree of the soil surface versus the forest stand is presented in Figure 20(a), and the corresponding percentage error is presented in Figure 20(b). The results are quite similar to those obtained in the last example. The estimated roughness degree seems exact compared to the ground truth value (0.11). For the forest with canopy thickness = 2.5 m, the error is almost zero, whereas the percentage error in the estimated roughness degree reaches about 0.3% for the forest region with canopy thickness = 5 m.

8. CONCLUSION

Electromagnetic simulation of PolSAR imaging together with SAR target decomposition using MSCM is applied to propose a method that employs PolSAR data for the estimation of a forest vertical structure. For electromagnetic simulation, the canopy layers of dense forest regions are modeled as clouds of randomly oriented thin straight dipoles with uniform random distribution within an inclined prism with horizontal rectangular base and parallelogram sides parallel to the direction of the incident plane wave. A new method is described to estimate the thickness of the canopy layer and the roughness of the soil surface. The proposed method is based on the RVI and RCS calculated from the PolSAR data and their relevance to the canopy layer thickness and ground roughness. Some examples are presented to demonstrate the capability of the proposed method using PolSAR image obtained through EM simulation of scattering from forest regions by applying the SAR target composition with MCSM. The proposed method is applied to estimate the forest vertical structure including the heights of the canopy layer bottom and top and the soil roughness for the simulated PolSAR images of the forest regions under investigation. The accuracy of the proposed method is assessed by calculating the percentage error of the estimated vertical structure and ground roughness for each resolution cell of the simulated forest region. It is shown that the percentage errors of the estimated parameters are very low, which reflects the accuracy and efficiency of the proposed method.

REFERENCES

1. Miner, R., "Impact of the global forest industry on atmospheric greenhouse gases," *Forestry, Food and Agriculture Organization of the United Nations*, Rome, 2010
2. Brigot, G., M. Simard, E. Colin-Koeniguer, and A. Boulch, "Retrieval of forest vertical structure from PolInSAR data by machine learning using LIDAR-derived features," *Remote Sensing*, Vol. 11, No. 4, 381, 2019.
3. Cloude, S. R. and K. P. Papathanassiou, "Three-stage inversion process for polarimetric SAR interferometry," *IEE Proceedings — Radar, Sonar and Navigation*, Vol. 150, No. 3, 125–134, 2003.
4. Neumann, M., L. Ferro-Famil, and A. Reigber, "Estimation of forest structure, ground, and canopy layer characteristics from multibaseline polarimetric interferometric SAR data," *IEEE Transactions on Geoscience and Remote Sensing*, Vol. 48, No. 3, 1086–1104, 2009.
5. Mette, T., F. Kugler, K. Papathanassiou, and I. Hajnsek, "Forest and the random volume over ground-nature and effect of 3 possible error types," *European Conference on Synthetic Aperture Radar (EUSAR)*, 1–4, VDE Verlag GmbH, 2006.
6. Zhou, Y.-S., W. Hong, and F. Cao, "An improvement of vegetation height estimation using multi-baseline polarimetric interferometric SAR data," *PIERS Online*, Vol. 5, No. 1, 6–10, 2009.
7. Kim, Y. and J. Zyl, "Comparison of forest estimation techniques using SAR data," *Proc. IEEE IGARSS Conf.*, 1395–1397, 2001.
8. Kim, Y., T. Jackson, R. Bindlish, S. Hong, G. Jung, and K. Lee, "Retrieval of wheat growth parameters with radar vegetation indices," *IEEE Geoscience and Remote Sensing Letters*, Vol. 11, No. 4, 808–812, 2014.

9. Huang, Y., J. P. Walker, Y. Gao, X. Wu, and A. Monerris, "Estimation of vegetation water content from the radar vegetation index at L-band," *IEEE Transactions on Geoscience and Remote Sensing*, Vol. 54, No. 2, 981–989, 2016.
10. Szigarski, T. Jagdhuber, M. Bau, C. Thiel, M. Parrens, J. Wignero, M. Piles, and D. Entekhabi, "Analysis of the radar vegetation index and potential improvements," *Remote Sensing*, Vol. 10, No. 11, 1776, 201.
11. Soliman, S. A. M., K. F. A. Hussein, and A.-E.-H. A. Ammar, "Electromagnetic resonances of natural grasslands and their effects on radar vegetation index," *Progress In Electromagnetics Research B*, Vol. 86, 19–38, 2020.
12. Papathanassiou, K. P. and S. R. Cloude, "Single-baseline polarimetric SAR interferometry," *IEEE Transactions on Geoscience and Remote Sensing*, Vol. 39, No. 11, 2352–2363, 2001.
13. Brandfass, M., C. Hofmann, J. C. Mura, J. R. Moreira, and K. P. Papathanassiou, "Parameter estimation of rain forest vegetation via polarimetric radar interferometric data," *SAR Image Analysis, Modeling, and Techniques IV*, Vol. 4543, 169–179, International Society for Optics and Photonics, January 2002.
14. Cloude, S. R., K. P. Papathanassiou, I. Woodhouse, J. Hope, J. C. Suarez Minguez, P. E. Osborne, and G. Wright, "The Glen Affric radar project: Forest mapping using polarimetric interferometry," *IGARSS 2001, Scanning the Present and Resolving the Future, Proceedings, IEEE 2001 International Geoscience and Remote Sensing Symposium (Cat. No.01CH37217)*, 2001.
15. Sarabandi, K. and Y. C. Lin, "Simulation of interferometric SAR response for characterizing the scattering phase center statistics of forest canopies," *IEEE Transactions on Geoscience and Remote Sensing*, Vol. 38, No. 1, 115–125, 2000.
16. Yang, H., D. Liu, G. Sun, Z. Guo, and Z. Zhang, "Simulation of interferometric SAR response for characterizing forest successional dynamics," *IEEE Geoscience and Remote Sensing Letters*, Vol. 11, No. 9, 1529–1533, 2014.
17. Freeman, A. and S. L. Durden, "A three-component scattering model for polarimetric SAR data," *IEEE Transactions on Geoscience and Remote Sensing*, Vol. 36, No. 3, 963–973, 1998.
18. Yamaguchi, Y., T. Moriyama, M. Ishido, and H. Yamada, "Four-component scattering model for polarimetric SAR image decomposition," *IEEE Transactions on Geoscience and Remote Sensing*, Vol. 43, No. 8, 1699–1706, 2005.
19. Zhang, L., B. Zou, H. Cai, and Y. Zhang, "Multiple-component scattering model for polarimetric SAR image decomposition," *IEEE Geoscience and Remote Sensing Letters*, Vol. 5, No. 4, 603–607, 2008.
20. Cloude, S. R. and E. Pottier, "A review of target decomposition theorems in radar polarimetry," *IEEE Transactions on Geoscience and Remote Sensing*, Vol. 34, No. 2, 498–518, Mar. 1996.
21. Maître, Henri, *Processing of Synthetic Aperture Radar (SAR) Images*, John Wiley & Sons, 2013.